nature geoscience

Supplementary information
https://doi.org/10.1038/s41561-025-01859-1

Future extreme precipitation amplified by intensified mesoscale moisture convergence

In the format provided by the authors and unedited

Inventory of Supporting Information

Future Extreme Precipitation Amplified by Intensified Mesoscale Moisture Convergence

Ping Chang[1,2*], Dan Fu[2*], Xue Liu[1], Frederic S. Castruccio[3], Andreas F. Prein[3,4], Gokhan Danabasoglu[3], Xiaoqi Wang[1], Julio Bacmeister[3], Qiuying Zhang[1], Nan Rosenbloom[3], Teagan King[3], Susan C. Bates[3,5]

Corresponding author: fudan1991@tamu.edu; ping@tamu.edu;

The Supporting Information includes:

Supplementary Figures 1-4
Supplementary Tables 1-3

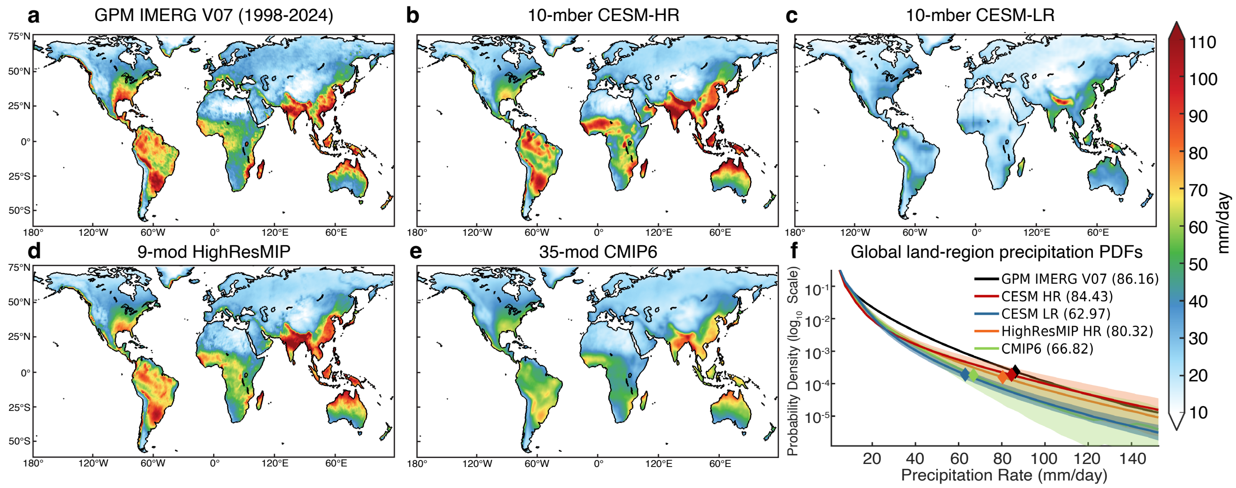

Supplementary Figure 1: Comparison of observed and simulated R99p using bilinear interpolation method. Similar to Fig. 1, but we compute R99p first on the model native grid and then interpolate to a common 1° × 1° grid using bilinear method. Shading in (f) shows ensemble spread (minimum–maximum range), and the diamond-shaped dots and numbers indicate precipitation values at the 99.9th percentile. The global mean R99p is 46.9 mm/day, 46.5 mm/day, 31.6 mm/day, 46.4 mm/day, and 39.5 mm/day, for IMERG V07, CESM-HR, CESM-LR, HighResMIP, and CMIP6, respectively. For PDFs, we interpolated all data first to 1° × 1° grid using bilinear method and then computed the probability density.

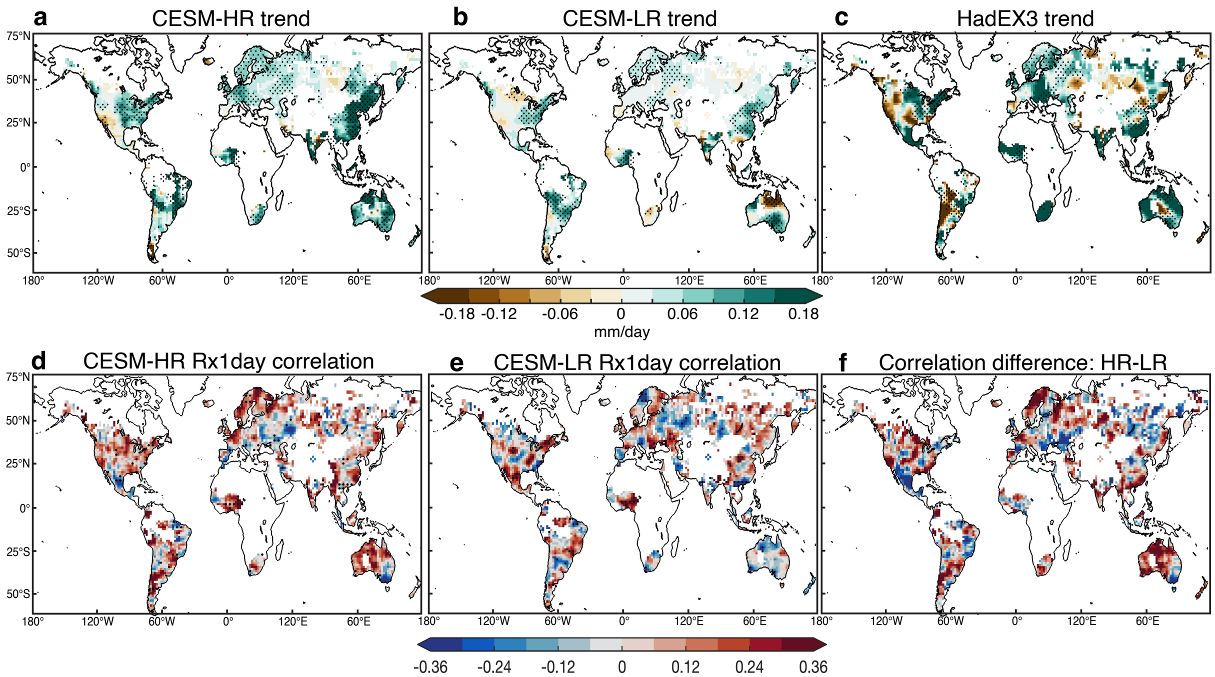

Supplementary Figure 2: Observed and simulated Rx1day trends and correlation. Rx1day trend from (a) CESM-HR, (b) CESM-LR, and (c) HadEX3, with stippling indicating regions where the trend is statistically significant at the 90% confidence level based on a Mann-Kendall test. Spearman rank correlation coefficients between HadEX3 and (d) CESM-HR, (b) CESM-LR, and (f) difference between CESM-HR and CESM-LR. Dots indicate region where the correlation coefficients are statistically significant at 90% confidence level.

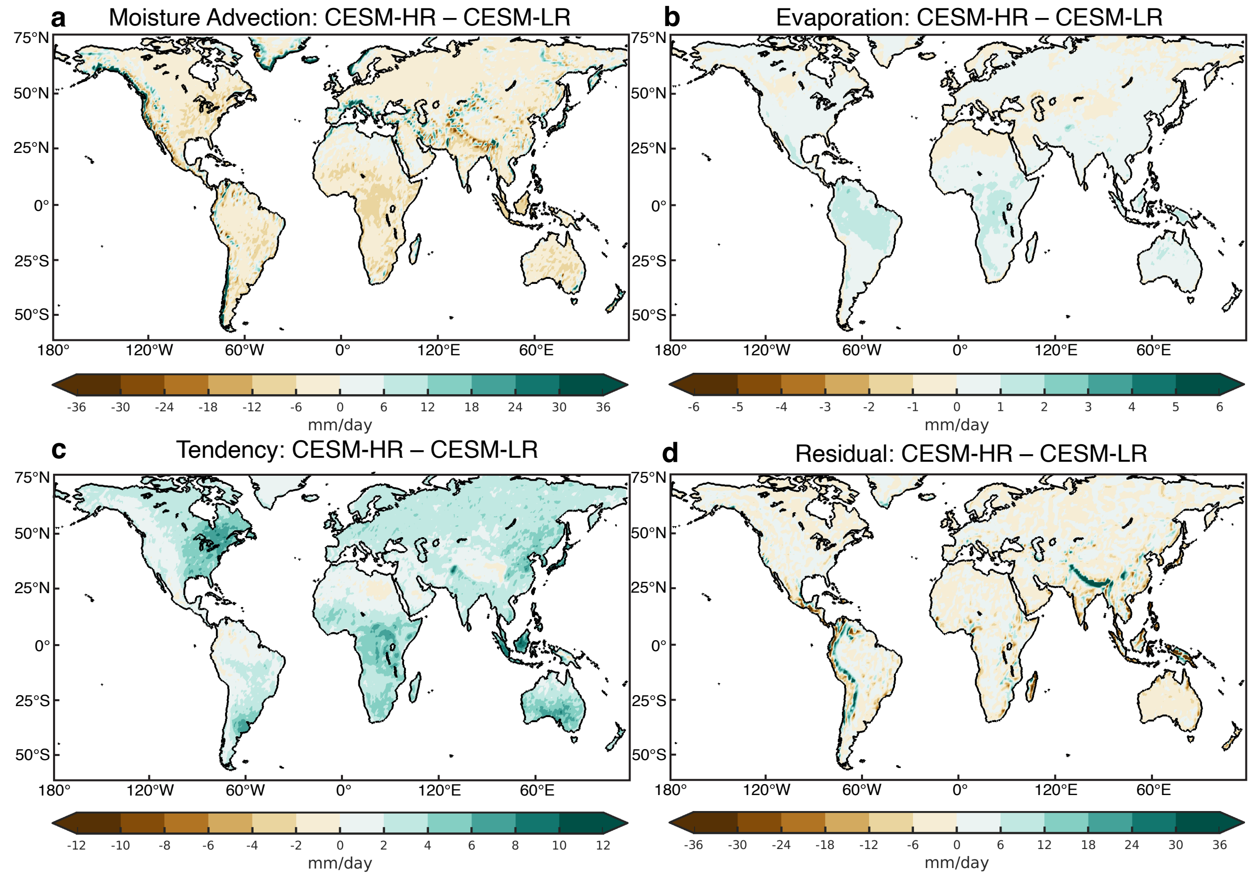

Supplementary Figure 3: Remaining moisture budget terms for Rx1day difference between CESM-HR and CESM-LR. (a) Contribution to the Rx1day difference between CESM-HR and CESM-LR from differences in moisture advection (M_a; $-\{\boldsymbol{u}\cdot\nabla q\}$). **(b)** As in **(a)**, but showing the contribution from differences in evaporation (E). **(c)** As in **(a)**, but showing the contribution from differences in moisture tendency (M_t; $\partial/\partial t\{q\}$). **(d)** As in **(a)**, but showing the contribution from the residual term. Note that different color scales are used for each term. Together with the dynamical tendency $M_{\Delta C}$ shown in Fig.2E and the thermodynamical tendency $M_{\Delta q}$ shown in Fig. 2F, these terms collectively describe the moisture budget contributing to the Rx1day difference between CESM-HR and CESM-LR. Among these terms, the dynamical tendency $M_{\Delta C}$ is clearly the most dominant process.

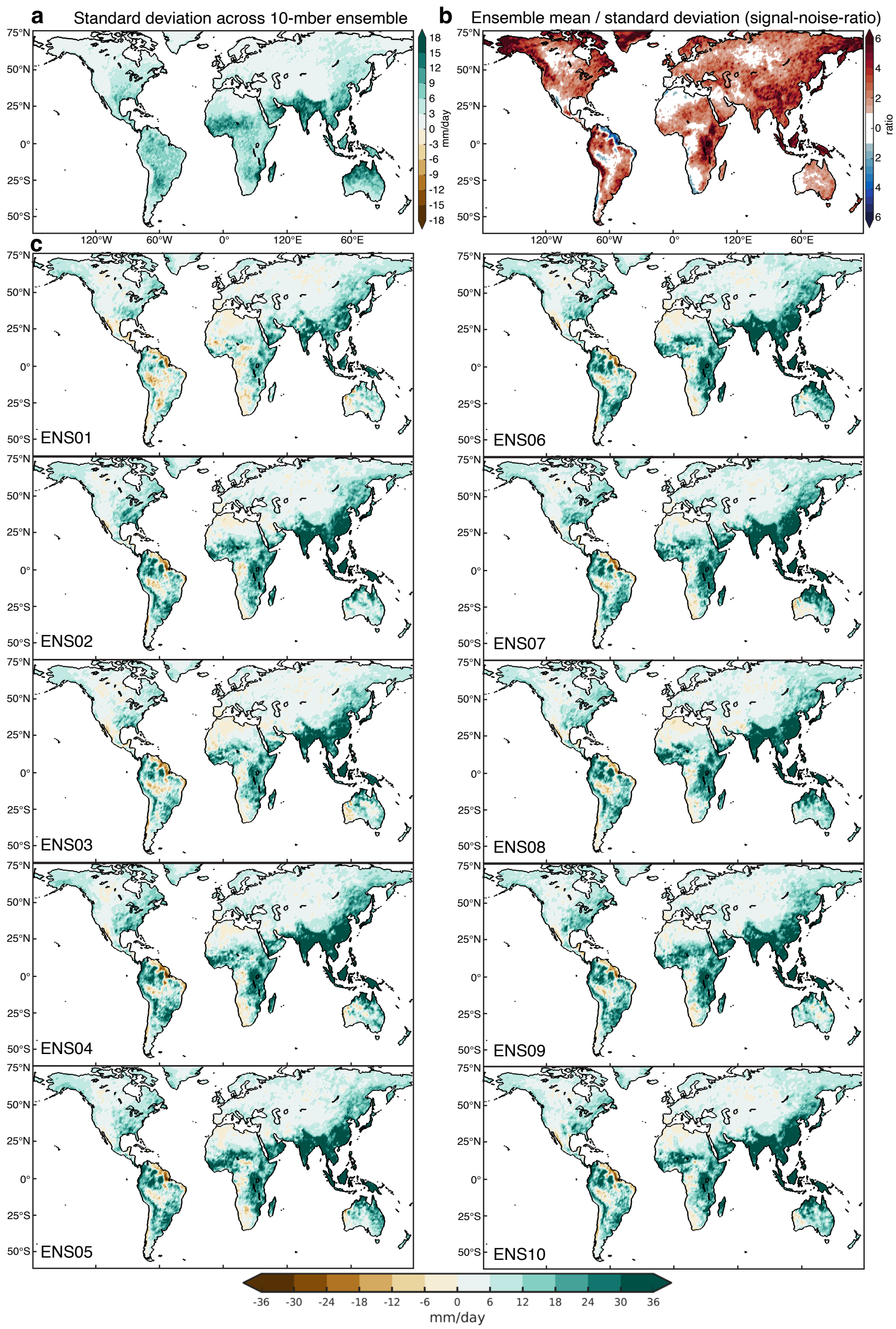

Supplementary Figure 4: Uncertainty quantification for projected Rx1day changes in CESM-HR. (**a**) Ensemble spread meansured by standard deviation (mm/day) across the 10 CESM-HR ensemble members, **(b)** Signal-to-noise ratio, defined as the ratio of the CESM-HR ensemble mean to its ensemble standard deviation, **(c)** Projected Rx1day changes (mm/day) calculated as the difference the future (2071-2100) and present (1981-2010) periods for each of the CESM-HR 10-member ensemble.

Supplementary Table 1: 35 CMIP6 models used for extreme precipitation computation

Model Name	Horizontal Resolution (lon. by lat. in degrees)	Institution
ACCESS-CM2	1.9° × 1.3°	Commonwealth Scientific and Industrial Research Organisation (CSIRO), Australia
ACCESS-ESM1-5	1.9° × 1.2°	
BCC-CSM2-MR	1.1° × 1.1°	Beijing Climate Center, China
BCC-ESM1	2.8° × 2.8°	
CanESM5	2.8° × 2.8°	Canadian Centre for Climate Modelling and Analysis, Canada
CESM2-FV2	1.3° × 0.9°	National Science Foundation National Center for Atmospheric Research, USA
CESM2	1.3° × 0.9°	
CESM2-WACCM-FV2	1.3° × 0.9°	
CESM2-WACCM	1.3° × 0.9°	
CNRM-CM6-1	1.4° × 1.4°	National Center for Meteorological Research, Météo-France and CNRS laboratory, France
CNRM-CM6-1-HR	0.5° × 0.5°	
CNRM-ESM2-1	1.4° × 1.4°	
EC-Earth3	0.7° × 0.7°	European Earth System Model, EU
EC-Earth3-Veg	0.7° × 0.7°	
FGOALS-f3-L	1.3° × 1°	Chinese Academy of Sciences, China
FGOALS-g3	2° × 2.3°	
GFDL-CM4	1° × 1°	U.S. Department of Commerce/National Oceanic and Atmospheric Administration (NOAA)/ Geophysical Fluid Dynamics Laboratory (GFDL), USA
GFDL-ESM4	1.3° × 1°	
HadGEM3-GC31-LL	1.9° × 1.3°	Met Office Hadley Centre, United Kingdom
HadGEM3-GC31-MM	0.8° × 0.6°	
INM-CM4-8	2° × 1.5°	Institute for Numerical Mathematics, Russia
INM-CM5-0	2° × 1.5°	
IPSL-CM6A-LR	2.5° × 1.3°	Institut Pierre-Simon Laplace, France
MIROC6	1.4° × 1.4°	Japan Agency for Marine-Earth Science and Technology (JAMSTEC), University of Tokyo (UT), National Institute for Environmental Studies (NIES) and RIKEN Center for Computational Science (R-CCS), Japan
MIROC-ES2L	2.8° × 2.8°	
MPI-ESM-1-2-HAM	1.9° × 1.9°	Max Planck Institute for Meteorology, Germany
MPI-ESM1-2-HR	0.9° × 0.9°	
MPI-ESM1-2-LR	1.9° × 1.9°	
MRI-ESM2-0	1.1° × 1.1°	Meteorological Research Institute, Japan
NESM3	1.9° × 1.9°	Nanjing University of Information Science and Technology, China
NorESM2-LM	2.5° × 1.9°	Norwegian Meteorological Institute, Norway
NorESM2-MM	1.1° × 0.9°	
SAM0-UNICON	1.3° × 0.9°	Seoul National University, South Korea
TaiESM1	1.3° × 0.9°	Research Center for Environmental Changes, Academia Sinica, Taiwan,
UKESM1-0-LL	1.9° × 1.3°	Met Office Hadley Center, United Kingdom

Supplementary Table 2: 9 HighResMIP models used for extreme precipitation computation

Model Name	Horizontal Resolution (lon. by lat. in degrees)	Institution
CESM-HR	0.25° × 0.25°	National Science Foundation National Center for Atmospheric Research, USA
CMCC-CM2-VHR4	0.31° ×0.23°	Euro-Mediterranean Centre on Climate Change, Italy
CNRM-CM6-1-HR	0.5° × 0.5°	National Center for Meteorological Research, Météo-France and CNRS laboratory, France
EC-Earth3P-HR	0.5° × 0.5°	European Earth System Model, EU
ECMWF-IFS-HR	0.23° ×0.23°	European Centre for Medium-Range Weather Forecasts (ECMWF)
FGOALS-f3-H	0.25° × 0.25°	Chinese Academy of Sciences, China
GFDL-CM4-HR	0.5° × 0.5°	U.S. Department of Commerce/National Oceanic and Atmospheric Administration (NOAA)/ Geophysical Fluid Dynamics Laboratory (GFDL), USA
HadGEM3-GC31-HM	0.35° × 0.23°	Met Office Hadley Center, United Kingdom
MPI-ESM1-2-XR	0.47° ×0.47°	Max Planck Institute for Meteorology, Germany

Supplementary Table 3: Sample sizes used to derive the spatial and temporal scales of atmospheric phenomena shown in Figure 3, tracked using the Multi-Object Analysis of Atmospheric Phenomena (MOAAP) program. For computational efficiency, only data from 2016–2020 were used for the scale analysis; however, the extensive sample size ensures that including additional years would not significantly change the results.

	Observation	CESM-HR	CESM-LR
Surface cyclones	950,521	1,045,962	777,296
Tropical cyclones	19,329	43,956	5,368
Mid-level cyclones	908,932	855,502	702,580
Anticyclones	796,158	844,807	655,783
MCSs	1,614,395	1,784,333	2,006
ARs	238,736	243,219	182,377
Jets	572,928	482,837	633,965
Equatorial Rossby waves	384,533	364,001	338
Mixed Rossby gravity waves	257,772	298,264	5,977
Kelvin waves	529,743	520,885	41,542
Inertia gravity waves	147,696	157,444	1,782
Eastward inertia gravity waves	351,225	334,438	16,324